

Optical transitions of Eu^{3+} ions in EuCl_3 solutions

S RAM, O P LAMBA and H D BIST

Department of Physics, Indian Institute of Technology, Kanpur 208 016, India

MS received 29 October 1983; revised 27 March 1984

Abstract. The optical absorption spectra of EuCl_3 in aqueous and acidic solutions were measured in the visible and uv regions of the spectrum. The concentration as well as the temperature of the solutions were varied to establish an accurate free-ion energy level scheme of Eu^{3+} . The energy levels were assigned on the basis of a correlation between the calculated and the experimentally observed transition energies and associated band intensities.

Keywords. Electronic energy levels; lanthanide ions; absorption spectroscopy; optical spectra; rare-earth ions.

PACS No. 78-40

1. Introduction

In view of technical and biological importance of rare-earth ions, recent years have seen a rapid growth of interest in the spectroscopic investigations of Eu^{3+} (Reisfeld and Jørgensen 1977). Most of the optical studies are concerned with transitions to or fluorescence from several 5D levels in the visible region of the spectrum. The energy level structure above 30000 cm^{-1} is essentially not very definite. Carnall *et al* (1968) made a complete theoretical calculation of the free-ion energy levels of Eu^{3+} (aquo) to 41600 cm^{-1} . These authors have also attempted the experimental investigation of these levels from the electronic absorption spectrum of Eu_2O_3 in perchloric acid. Similar studies on $\text{Eu}(\text{C}_2\text{H}_5\text{SO}_4)_3 \cdot 9\text{H}_2\text{O}$ (Hellwege *et al* 1957, 1963) Eu^{3+} : LaCl_3 (Dieke 1968; Dieke and Crosswhite 1963) and $\text{EuP}_5\text{O}_{14}$ (Sekita *et al* 1980) in single crystals are also available in literature.

This paper presents a complete visible and uv electronic-absorption study of EuCl_3 in aqueous and acetic acid solutions. Both the concentration as well as the temperature of the solution have been varied to avoid ambiguity from the bands of unionized molecular species (Chrysochoos 1974; Habenschuss and Spedding 1980) or the thermally excited bands from 7F_1 and 7F_2 levels (which lie $\sim 360\text{ cm}^{-1}$ and $\sim 1050\text{ cm}^{-1}$, respectively, above the ground level 7F_0). The assignment of the observed bands to various electronic transitions arising from the ground state 7F_0 and the first excited state 7F_1 to 5D and other excited levels of Eu^{3+} is made by comparing the experimental transition energies and band intensities with theoretical values reported by Carnall *et al* (1965, 1968) and Carnall and Fields (1967).

2. Experimental details

The specpure sample of $\text{EuCl}_3 \cdot 6\text{H}_2\text{O}$ was obtained commercially from Ventran Alfa Products, USA, and used as received. The aqueous and acidic solutions were prepared by

dissolving $\text{EuCl}_3 \cdot 6\text{H}_2\text{O}$ in triple distilled water and dry glacial acetic acid, respectively. The absorption spectra of concentrated and dilute solutions were obtained in the visible and uv regions of the spectrum on a Cary-17D spectrophotometer using optical cells of length 1, 5 and 10 cm. In our experiments, the concentration of the solutions could not be varied more than 50–1000 folds for aqueous and 50 folds for the acid solution as the band intensities of Eu^{3+} are very poor (as compared to other lanthanide ions) and also the solubility of EuCl_3 in both these solvents is very small. The temperature of the aqueous solution was varied from 273–343 K and controlled within ± 2 K by circulating water in a water-bath through the sample and solvent holders.

Absorption bands of Eu^{3+} are superposed on a strong absorption-background which in general increases to the shorter wavelength side and becomes more dominant at lower concentrations and in acetic-acid solutions. Moreover, the spectrum below 400 nm in acidic solutions becomes diffuse and the general absorption dominates over the characteristically sharper bands of the ion; and thus acetic acid is not a proper solvent for the absorption studies below this region. In the present study, this absorption background is subtracted to report the absorbances of the observed bands and attempts have been made to develop even the weak and broad bands by suppressing the general background. The final spectra were run at 15, 6, 1.5 nm/inch dispersion, 0.01–0.005 nm/sec chart-speed, 1 or 5 sec pen period, 0.02–0.005 mm slit-width and 0.10–0.02 nm spectral band-width, according to the intensities and natural widths of the absorption bands. Furthermore, to resolve the crystal field splitting in a few sharp bands, the spectra were recorded at a somewhat higher dispersion, *i.e.*, 0.3 nm/inch. The reported frequencies are accurate to $\pm 5 \text{ cm}^{-1}$ for the sharp and intense bands and $\pm 10 \text{ cm}^{-1}$ (or even more) for the weak, diffuse and broad bands.

3. Results and discussion

We have measured the optical absorption spectra (650–200 nm) of EuCl_3 in the aqueous and acidic solutions at different temperatures and concentrations. The absorption spectra of aqueous solution at two extreme temperatures 273 K and 343 K are shown in figure 1. The transition energies, molar absorptivities ϵ ($\text{mol}^{-1} \text{ l cm}^{-1}$) and oscillator strengths f of the observed bands together with the assigned transitions are summarized in table 1. λ_{air} is the wavelength (nm) in air of the peak for a band and ν_{vac} is the corresponding wavenumber (cm^{-1}) in vacuum. Conversion of λ_{air} to ν_{vac} is made through a standard wavenumber table of Coleman *et al* (1960). A few characteristic features of the spectra studied are given below:

(i) Absorption bands appearing in the 600–400 nm region are relatively weak and have absorbances in the range 0.0007 to 0.098 $\text{mol}^{-1} \text{ l cm}^{-1}$. (ii) More intense and broad bands are observed in 400–240 nm region (molar absorbance changes between 0.005 to 2.8 $\text{mol}^{-1} \text{ l cm}^{-1}$). (iii) The excitations from the ground state 7F_0 are usually sharp but those from the excited level 7F_1 are relatively broad, diffuse and weak. (iv) Bands involving 7F_0 state are almost independent of temperature and concentration. However, the hypersensitive bands identified at 525, 464 and 415 nm for the ${}^7F_0 \rightarrow {}^5D_1$, ${}^7F_0 \rightarrow {}^5D_2$ and ${}^7F_1 \rightarrow {}^5D_3$ transitions, respectively, are very sensitive to concentration for their intensities. The bands excited from thermally populated state 7F_1 do seem to enhance at higher temperatures. The change of concentration exhibits very little effect but no regular pattern between concentration and intensity was noted.

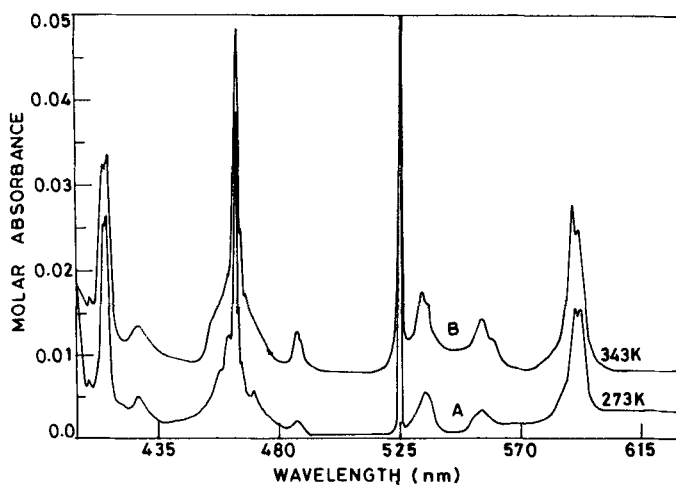


Figure 1a. Absorption spectra of Eu^{3+} in an aqueous solution (0.368 mol/l) of $\text{EuCl}_3 \cdot 6\text{H}_2\text{O}$; (A) at 273 K and (B) at 343 K in the range 630 to 400 nm.

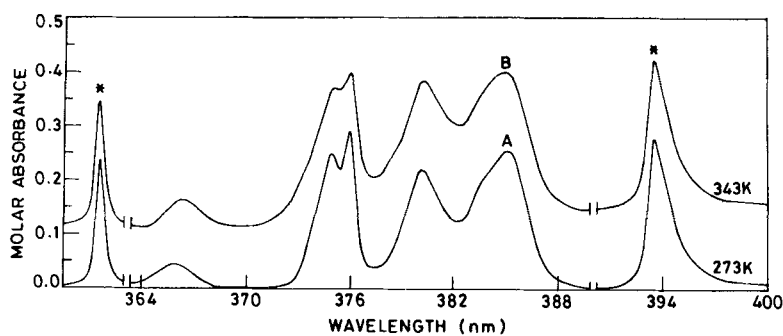


Figure 1b. Absorption spectra of Eu^{3+} corresponding to those of figure (1a) in the range 400 to 360 nm. The actual absorbances of 394 and 361 nm bands (indicated by *) are 10 and 2 times, respectively, to those shown in the figure.

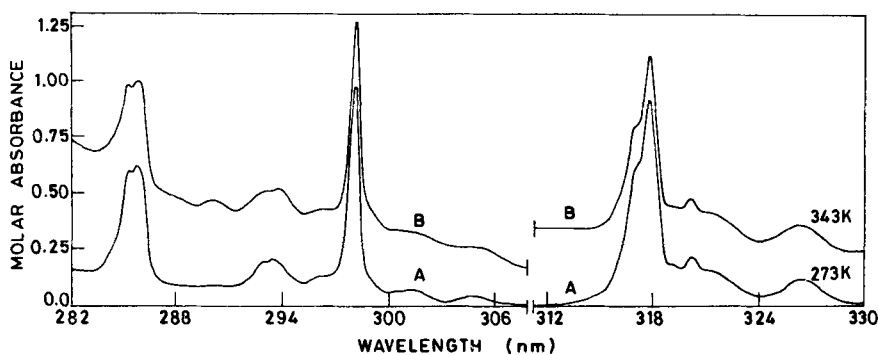


Figure 1c. Absorption spectra of Eu^{3+} corresponding to those of figure (1a) in the range 330 to 282 nm.

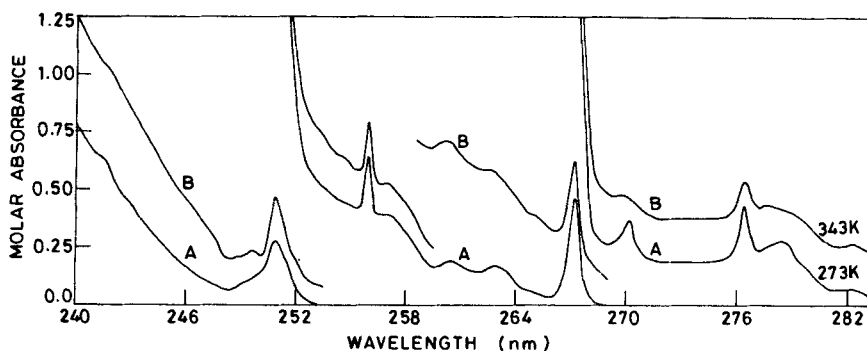


Figure 1d. Absorption spectra of Eu^{3+} corresponding to those of figure (1a) in the range 283 to 240 nm. The absorbance scale given applies for the middle spectrum (270–252 nm). This scale has to be multiplied by 0.2 and 4 for the regions 283–268 nm and 253–240 nm, respectively.

(v) The characteristically sharp transitions of Eu^{3+} are superposed on a continuous increasing general absorption background towards the shorter wavelength side. This background, at lower concentrations or at higher temperatures and in the acidic solutions, becomes more and more dominant. Moreover, in acetic acid, the spectrum below 400 nm becomes diffuse and the general absorption intensity dominates over the intensities of $4f \rightarrow 4f$ bands, and therefore it is not a suitable solvent for absorption studies below this region. The actual cause of the general absorption in lanthanides is not known so far (Heller 1968; Carnall *et al* 1968; Gschneidner and Eyring 1979).

The oscillator strengths, f , of the bands observed were calculated from the integral area under the absorption curves using the expression

$$f = 4.32 \times 10^{-9} \int \epsilon \cdot d\nu$$

Since the shapes of Eu^{3+} -bands (shown in figure 1) are neither pure Lorentzian nor pure Gaussian, the area within the absorption bands were estimated from the graphical method, integrating over the entire band plotted in frequency scale. The extinction coefficients ϵ ($\text{mol}^{-1} \text{l cm}^{-1}$) were obtained from $\epsilon = A/Cl$, where A is the absorbance and is read directly from the spectrum, C is the concentration of the solution in mol/l , and l is the cell length in cm.

The $4f \rightarrow 4f$ electronic transitions in Eu^{3+} and other lanthanide ions are forbidden on the basis of pure electric dipole [$\Delta S = 0$, $\Delta J = 0, \pm 1$ (but $J_1 = J_2 \neq 0$) and $\Delta L = \pm 1$] and magnetic dipole ($\Delta S = 0$, $\Delta J \leq 1$ and $\Delta L = 0$) selection rules (Gschneidner and Eyring 1979). The transition $J_1 = 0 \rightarrow J_2 = 0$ is absolutely forbidden, not only for the electric-dipole transition but for any kind of multipole transition. In fact, in the lanthanides two energy levels with same J mix their two differing S values as a result of the strong spin-orbit coupling, and thus the spin selection rule $\Delta S = 0$ remains no longer valid. The absorption bands which are experimentally observed usually acquire their intensities from the forced (a) magnetic dipole, (b) electric dipole and (c) electric-quadrupole transitions.

3.1 Magnetic dipole transitions

${}^7F_0 \rightarrow {}^7F_1$ and ${}^7F_1 \rightarrow {}^7F_2$ are the two pure magnetic dipole transitions of Eu^{3+} and fall

Table 1. Electronic transitions of Eu^{3+} observed in the absorption spectrum of aqueous solution (0.368 mole/l) of $\text{EuCl}_3 \cdot 6\text{H}_2\text{O}$ at 298 K.

λ_{air} (nm) 1	ν_{vac} (cm^{-1}) 2	$10^3 \epsilon$ ($\text{mol}^{-1} \text{l cm}^{-1}$) 3	$10^8 f$ (mol^{-1}) 4	Assignment 5	
591	16916 [16923]	15.4	1.13	${}^7F_1 \rightarrow {}^5D_0$	
589	16973 [16973]	15.0			
578.8**	17272** [17263]	97.8**	0.51**	${}^7F_0 \rightarrow {}^5D_0$	(7)
554.1*	18042*	1.6			
552.1*	18108*	1.4	0.35	${}^7F_2 \rightarrow {}^5D_1$	
538.0	18582	3.5			
534.5	18704 [18650]	5.8	0.47	${}^7F_1 \rightarrow {}^5D_1$	
532.5	18774	6.5			
525.54	19023	72			
525.20	19035 [19030]	97	1.60	${}^7F_0 \rightarrow {}^5D_1$	(8)
524.90	19046	75			
487.5*	20507*	2.0			
486.0*	20570*	2.2	0.25	${}^7F_2 \rightarrow {}^5D_2$	
471.2	21216	6.6	0.20	${}^7F_1 \rightarrow {}^5D_2$	
465.51	21476	10			
464.56	21520	36			
464.32	21531	35	1.33	${}^7F_0 \rightarrow {}^5D_2$	(9)
463.93	21549	21			
463.74	21558	10			
429.40*	23282*	1.6			
428.20*	23347*	3.0	0.40	${}^7F_2 \rightarrow {}^5D_3$	
416.4	24009	22			
415.4	24066	20	2.40	${}^7F_1 \rightarrow {}^5D_3$	
414.1	24142	17			
410.0	24383	0.7	0.01	${}^7F_0 \rightarrow {}^5D_3$	(10)
398.6	25081	70	4	${}^7F_1 \rightarrow {}^5L_6$	
396.6*	25207*	400			
394.01*	25373*	2260	137	${}^7F_0 \rightarrow {}^5L_6$	(11)
393.56*	25402*	2760			
387.15	25822	50	d	${}^7F_0 \rightarrow {}^5G_2$	(12)
385.05	25963	255	d	${}^7F_0 \rightarrow {}^5G_2$	
384.05*	26031*	220	d	${}^7F_0 \rightarrow {}^5L_7$	(13)
383.46*	26071*	200	d	${}^7F_0 \rightarrow {}^5L_7$	
381.01*	26239*	170		${}^7F_1 \rightarrow {}^5G_4$	
379.98	26310	225	d	${}^7F_1 \rightarrow {}^5G_5$	
378.35*	26423*	75		${}^7F_0 \rightarrow {}^5G_3$	(14)
375.71	26609	300		${}^7F_0 \rightarrow {}^5G_4$	(15)
374.62*	26686*	250	21.2	5G_5	(16)
373.35	26777	100		5G_6	(17)
366.35	27289	55	4.6	${}^7F_1 \rightarrow {}^5D_4$	
(364.40)	(27435)	—	—	${}^7F_0 \rightarrow {}^5L_8$	(18)

Table 1. (Contd.)

1	2	3	4	5	
361.57	27649	578	12.7	${}^7F_0 \rightarrow {}^5D_4$	(19)
(353.96)	(28244)	—	—	${}^7F_0 \rightarrow {}^5L_9$	(20)
(346.96)	(28813)	—	—	${}^7F_0 \rightarrow {}^5L_{10}$	(21)
328.15	30465	20			
327.24	30550	81	4.2	${}^7F_1 \rightarrow {}^5H_7$	
326.32	30636	110			
325.50*	30713*	85	0.5	${}^7F_0 \rightarrow {}^5H_3$	(22)
322.70	30980	90		${}^7F_1 \rightarrow {}^5H_5$	
321.37	31108	150		5H_6	
320.22*	31220*	210	11.5	${}^7F_0 \rightarrow {}^5H_7$	(23)
319.24	31315	175		5H_4	(24)
318.0*	31437*	910		${}^7F_0 \rightarrow {}^5H_5$	(25)
317.3	31507	620 (sh)	65.5	5H_6	(26)
306.3*	32638*	25		${}^7F_1 \rightarrow {}^5F_2$	
305.5*	32724*	45	7.0	5F_3	
304.8*	32798*	50		${}^7F_0 \rightarrow {}^3P_0$	(27)
302.6	33037	25		${}^7F_0 \rightarrow {}^5F_2$	(28)
302.3	33071	30			
301.4*	33169*	50	5.0	${}^7F_0 \rightarrow {}^5F_3$	(29)
300.6	33257	48		${}^7F_1 \rightarrow {}^5F_4$	
298.8*	33457*	95 (sh)	0.5	${}^7F_0 \rightarrow {}^5F_1$	(30)
298.00	33547	915	29.5	${}^7F_0 \rightarrow {}^5F_4$	(31)
295.9	33785	90			
295.5	33831	70	3.5	${}^7F_1 \rightarrow {}^5F_5$	
294.1*	33992*	90 (sh)		${}^7F_0 \rightarrow {}^5I_5$	(32)
293.3	34085	160			
292.8	34143	140	18.0	${}^7F_1 \rightarrow {}^5(IH)_5$	
292.1*	34224*	75 (sh)		${}^7F_0 \rightarrow {}^5F_5$	(33)
290.7*	34390*	15			
290.0*	34472*	20	0.8	${}^7F_0 \rightarrow {}^5(IH)_5$	(34)
288.8*	34616*	10	0.3	${}^7F_1 \rightarrow {}^5I_8$	
287.6*	34760*	15	0.5	${}^7F_1 \rightarrow {}^5(IH)_6$	
286.56	34887	60 (sh)	1.5	${}^7F_1 \rightarrow {}^5I_7$	
285.71*	34990*	515			
285.26*	35045*	490	40.4	${}^7F_0 \rightarrow {}^5I_8$	(35)
284.4	35151	163			
283.9	35213	63	10.0	${}^7F_0 \rightarrow {}^5(IH)_6$	(36)
283.5	35263	25			
282.4*	35400*	30	d	${}^7F_0 \rightarrow {}^5I_7$	(37)
279.2	35806	45			
278.1	35948	50	bd	${}^7F_1 \rightarrow {}^5K_5$	
277.3	36051	40			
276.4	36170	50	2.5	${}^7F_0 \rightarrow {}^5K_5$	(38)
270.6	36944	30			
270.2	36999	45	d	${}^7F_1 \rightarrow {}^5K_6$	

Table 1. (Contd.)

1	2	3	4	5	
267.3	37400	450	17.2	${}^7F_0 \rightarrow {}^5K_6$	(39)
263.5	37939	65		${}^7F_1 \rightarrow {}^5K_7$	
262.6*	38069*	60	d	${}^7F_0 \rightarrow {}^3P_1$	(40)
261.2	38273	12		${}^7F_1 \rightarrow {}^5G_2$	
260.5	38376*	35	d	${}^7F_0 \rightarrow {}^5K_7$	(41)
259.2	38569	5		${}^7F_1 \rightarrow {}^5K_8$	
258.5*	38673*	40		${}^7F_0 \rightarrow {}^5G_2$	(42)
257.9*	38763*	85	12	${}^7F_1 \rightarrow {}^3(KI)_6$	(43)
256.9*	38914*	90		${}^7F_0 \rightarrow {}^5K_8$	
255.93	39062	275	9	${}^7F_0 \rightarrow {}^3(KI)_6$	(44)
254.8	39235	10		${}^7F_0 \rightarrow {}^5G_3$	(45)
254.3	39312	5		${}^7F_1 \rightarrow {}^5(DP)_2$	
253.7*	39405*	10	nc	5K_9	
253.1*	39498*	20		5G_4	
252.1	39655	300 (sh)		${}^7F_0 \rightarrow {}^5(DP)_2$	(46)
251.6*	39734*	850 (sh)		5K_9	(47)
250.9	39845	1160	130	5G_4	(48)
249.9	40004	450 (sh)		${}^5(DP)_3$	(49)
249.3	40100	350	15	${}^7F_1 \rightarrow {}^5G_5$	
(247.05)	(40465)	—	—	${}^7F_0 \rightarrow {}^5G_5$	(50)
243.1*	41123*	ewd	—	${}^7F_0 \rightarrow {}^5D_1$	(51)
(241.89)	(41329)	—	—	${}^7F_0 \rightarrow {}^3O_{10}$	(52)
241.4	41412	ewd	—	${}^7F_0 \rightarrow {}^5G_6$	(53)
(239.95)	41663	—	—	${}^7F_0 \rightarrow {}^3H_5$	(54)

* Absorption bands of Eu^{3+} not observed previously in the solution spectra of the related compounds [Carnall *et al* (1968); Heller (1968)]. ** Band observed in CH_3COOH solution [concentration = $0.0031 \text{ mol l}^{-1}$]. Note: (a) The quantities within parentheses in column no. 1-2 refer to the electronic transitions of Eu^{3+} calculated theoretically [Carnall *et al* (1968)]. (b) The frequencies (cm^{-1}) written within the square brackets in column no. 2 are the corresponding values obtained from our fluorescence data in aqueous solution. (c) The numbers within parentheses in the last column denote the serial numbers of the principal electronic transitions occurring from the ground state (7F_0) to different excited levels. (d) d = diffuse, bd = broad and diffuse, sh = shoulder, ewd = extremely weak and diffuse, nc = not very certain. (e) Extinction coefficients ϵ and oscillator strengths f of the observed bands do not include the general-absorption background.

at ~ 360 and $\sim 700 \text{ cm}^{-1}$, respectively (Dieke 1968). The other transitions of Eu^{3+} which show magnetic dipole characters are the force-induced magnetic dipole transitions, which usually satisfy the selection rules

$$\Delta S \neq 0, \Delta L = 0, \pm 1; \Delta J \leq 1 \text{ and } \Delta I = 0.$$

The absorption bands observed at 525 and 299 nm attribute to ${}^7F_0 \rightarrow {}^5D_1$ and ${}^7F_0 \rightarrow {}^5F_1$ transitions, both of which are the magnetic dipole transitions of the latter type. Carnall *et al* (1968) have calculated the magnetic-dipole oscillator strengths for these two bands as 1.62×10^{-8} and 2.16×10^{-8} , respectively. In the present

experimental investigation these values were found as 1.60×10^{-8} and 0.5×10^{-8} , respectively. Incomparably large theoretical intensity of the latter band lies in the approximation of one-electron nature of the effective interaction with the open shell electrons which, of course, is not well justified. Newman *et al* (1982, 1983) have attempted to include also the effects of two-electron interactions.

The transitions from the thermally excited level 7F_1 giving rise to the bands at 590 and 306 nm have an oscillator strength of about 1.1×10^{-8} and 7.0×10^{-8} and have been assigned for the ${}^7F_1 \rightarrow {}^5D_0$ and ${}^7F_1 \rightarrow {}^5F_2$ transitions, respectively. Both these transitions obey the selection rules for a magnetic dipole transition. Sage *et al* (1979), on the basis of magnetic circular dichroism spectra of aqueous EuCl_3 , have confirmed ${}^7F_1 \rightarrow {}^5D_0$ as an electric quadrupole transition. On the other hand, the structure of ${}^7F_1 \rightarrow {}^5F_2$ band is obscured by the neighbouring bands and the general absorption background; thus no further elucidation of its nature seems possible.

3.2 Forced-electric dipole transitions

In general, the strong $4f \rightarrow 4f$ absorption bands (oscillator strengths $\approx 10^{-5}$ – 10^{-8}) of lanthanides are attributed to the forced electric dipole transitions. These transitions gain the additional intensities from (a) the ligand-field produced at the RE^{3+} site by the surrounding ionic species and/or (b) from the vibronic interactions of molecular complexes of RE^{3+} in solution and also in solid (Habenschuss and Spedding 1979; 1980; Gschneidner and Eyring 1979). In both kinds of forced electric-dipole transitions, the selection rules allowed from the other regions allow J to change at most 6 units (Gschneidner and Eyring 1979) and most of the Eu^{3+} -bands listed in table 1 appear as the result of these transitions. The 394 nm band of EuCl_3 , assigned for ${}^7F_0 \rightarrow {}^5L_6$ transition, is the most intense band among all its known transitions and provides a good example in which the bands associated with $\Delta J = 6$ exhibit a maximum intensity. The medium strong band at 361 nm and weak band at 366 nm [see figure (1b)] are likewise immediately assigned to ${}^7F_0 \rightarrow {}^5D_4$ and ${}^7F_1 \rightarrow {}^5D_4$, respectively. The transition ${}^7F_0 \rightarrow {}^5I_8$ violates the selection rule $\Delta J \leq 6$, but appears with an appreciably large intensity. The other transitions which also do not follow this selection rule but occur strongly are ${}^7F_0 \rightarrow {}^5(IKL)_7$, ${}^7F_{0,1} \rightarrow {}^5K_9$ and ${}^7F_1 \rightarrow {}^5K_8$ (see table 1). In fact, the electronic states of lanthanide ions as derived using Russell-Saunders coupling scheme are not the pure states, and as a consequence ΔJ and ΔL do not follow any rigorous selection rule in $4f \rightarrow 4f$ transitions, and the one-electron model under the assumption of which these rules are derived is not sufficient (Newman 1982 and 1983) to reproduce the experimental results.

3.3 Electric-quadrupole and hypersensitive transitions

The electric-quadrupole transitions occur between the states of the same parity and J changes at most 2 units. But these transitions in general are extremely weak having the oscillator strengths of $\sim 10^{-8}$ – 10^{-9} . The absorption band observed at 590 nm in the aqueous as well as the acidic solutions corresponds to ${}^7F_1 \rightarrow {}^5D_0$ transition and has also been taken as an example of such an electric-quadrupole transition (Sage *et al* 1979). It is interesting and rather easy to understand why the transition ${}^7F_0 \rightarrow {}^5D_1$ retains its pure magnetic dipolar character and the ${}^7F_1 \rightarrow {}^5D_0$ exhibits an electric quadrupolar character, while both follow the same selection rule $\Delta J = \pm 1$. In fact, the quadrupole

intensity of a 0–1 transition depends on the mixing of $J = 0$ and $J = 1$ states through an intermediate state with $J = 2$. For the transition ${}^7F_1 \rightarrow {}^5D_0$, the nearest levels that can give $\Delta J = 2$ character after mixing differ by $\sim 700 \text{ cm}^{-1}$ (difference between 7F_1 and 7F_2 levels) while for the ${}^7F_0 \rightarrow {}^5D_1$ transition the corresponding levels (*i.e.* 5D_1 and 5D_2) differ by about 2500 cm^{-1} .

The weak absorption bands observed at 554, 486 and 429 nm have almost the similar band structures and band intensities (oscillator strengths 0.35×10^{-8} , 0.25×10^{-8} and 0.40×10^{-8} respectively), and thus seem to belong to the same series of electronic transitions of the Eu^{3+} ions. The observed energy values are comparable to the energy differences of 5D_1 , 5D_2 and 5D_3 levels with respect to the excited level 7F_2 . Though the Boltzmann population of 7F_2 level at the temperatures employed in our experiments is very small (roughly 10^{-3} times to that for the ground state 7F_0), on the basis of energy correlations all three bands have been assigned for ${}^7F_2 \rightarrow {}^5D_1$, ${}^7F_2 \rightarrow {}^5D_2$ and ${}^7F_2 \rightarrow {}^5D_3$ transitions respectively. Due to extremely small intensity, no further elucidations regarding their spectral changes with respect to the changes of concentration and temperature could be inferred.

The experimental intensities of a few electric quadrupole transitions are as high as $\sim 10^4$ times the calculated intensities and are very sensitive to the environment about the ion (Peacock 1975, 1977). These hypersensitive transitions are called pseudoelectric quadrupole transitions. The electronic transitions ${}^7F_0 \rightarrow {}^5D_2$ and ${}^7F_1 \rightarrow {}^5D_3$, which appear at 464 and 415 nm, have the oscillator strengths 1.33×10^{-8} and 2.40×10^{-8} , respectively, in the aqueous solution. Intensities of both bands have been noted to increase by a factor of ~ 10 in going from aqueous to acidic solution. Moreover, the magnetic-dipole transition ${}^7F_0 \rightarrow {}^5D_1$ appearing at 525 nm has also been observed to show similar features. The detailed studies regarding the hypersensitive characters of these bands are in progress and will be published separately.

4. Conclusions

The optical absorption studies of Eu^{3+} in aqueous and acidic solutions of EuCl_3 as a function of concentration and temperature provide a better understanding of the $4f \rightarrow 4f$ transitions of Eu^{3+} originated from 7F_0 and 7F_1 levels. The intensities of hypersensitive bands identified at 525, 464 and 415 nm for the electronic transitions ${}^7F_0 \rightarrow {}^5D_1$, ${}^7F_0 \rightarrow {}^5D_2$ and ${}^7F_1 \rightarrow {}^5D_3$, respectively, show a considerable increase in going from aqueous to acidic solutions and thus suggest a larger ligand-field strength at Eu^{3+} site in the acidic solutions. Moreover, a prominent appearance of ${}^7F_0 \rightarrow {}^5D_0$ band at 578 nm (which is forbidden through an electric-dipole and also in other electric-multipole transitions) in the acidic solutions and its total disappearance in the aqueous solutions reveal that the site symmetries of Eu^{3+} in these two solvents are essentially not the same.

Acknowledgements

The authors thank Mr R K Jain for his valuable help in recording the absorption spectra. Financial assistance received from DST, New Delhi, India is gratefully acknowledged.

References

- Carnall W T and Fields P R 1967 *Adv. Chem. Ser.* **71** 86
Carnall W T, Fields P R and Rajnak K 1968 *J. Chem. Phys.* **10** 4412, 4450
Carnall W T, Fields P R and Wybourne B G 1965 *J. Chem. Phys.* **42** 3797
Chrysochoos J 1974 *J. Chem. Phys.* **60** 1110
Coleman C D, Bozman W R and Meggers W F 1960 *Table of wavenumbers* (Washington: National Bureau of Standards)
Dieke G H 1968 *Spectra and energy levels of rare-earth ions in crystals* (New York: John Wiley)
Dieke G H and Crosswhite H M 1963 *Appl. Opt.* **2** 675
Deshazer L G and Dieke G H 1963 *J. Chem. Phys.* **38** 2190
Gschneidner K A and Eyring L 1979 *Hand book of physics and chemistry of rare earths* (New York, Elsevier: North-Holland)
Habenschuss A and Spedding F H 1979 *J. Chem. Phys.* **70** 2797
Habenschuss A and Spedding F H 1980 *J. Chem. Phys.* **73** 442
Heller A 1968 *J. Mol. Spectrosc.* **20** 208
Hellwege K H, Johnsen U, Kahle H G and Schaak G 1957 *Z. Phys.* **148** 112
Hellwege K H, Hufner S and Pocker A 1963 *Z. Phys.* **172** 453
Newman D J, Siu G G and Fung W Y P 1982 *J. Phys.* **C15** 3113
Newman D J 1983 *J. Phys. F.* **13** 1511
Peacock R D 1975 *Struct. Bond* **22** 83
Peacock R D 1977 *Mol. Phys.* **33** 1239
Reisfeld R and Jørgensen C K 1977 *Lasers and excited states of rare earths* (New York: Springer-Verlag)
Sage M L, Buonocore M H and Pink H S 1979 *Chem. Phys. Lett.* **36** 171
Sekita M, Minami F, Okamoto E and Masui H 1980 *Phys. Status Solidi* **b101** 353